

## Estimation of Arrival Time of Coronal Mass Ejections in the Vicinity of the Earth Using Solar and Heliospheric Observatory and Solar TERrestrial RELations Observatory Observations

Anitha Ravishankar<sup>1</sup> · Grzegorz Michalek<sup>1</sup>

© Springer ●●●

**Abstract** The arrival time of coronal mass ejections (CMEs) in the vicinity of the Earth is one of the most important parameters in determining space weather. We have used a new approach to predicting this parameter. First, in our study, we have introduced a new definition of the speed of ejection. It can be considered as the maximum speed that the CME achieves during the expansion into the interplanetary medium. Additionally, in our research we have used not only observations from the *SOLar and Heliospheric Observatory* (SOHO) spacecraft but also from *Solar TERrestrial RELations Observatory* (STEREO) spacecrafts. We focus on halo and partial-halo CMEs during the ascending phase of Solar Cycle 24. During this period the STEREO spacecraft were in quadrature position in relation to the Earth. We demonstrated that these conditions of the STEREO observations can be crucial for an accurate determination of transit times (TT) of CMEs to the Earth. In our research we defined a new initial velocity of CME, the maximum velocity determined from the velocity profiles obtained from a moving linear fit to five consecutive height–time points. This new approach can be important from the point of view of space weather as the new parameter is highly correlated with the final velocity of ICMEs. It allows one to predict the TTs with the same accuracy as previous models. However, what is more important is the fact that the new approach have radically reduced the maximum TT estimation errors to 29 hours. Previous studies determined the TT with a maximum error equal 50 hours.

**Keywords:** Sun: coronal mass ejections (CMEs) . Sun: Space Weather

---

✉ Ravishankar  
anitha@oa.uj.edu.pl  
Michalek  
grzegorz.michalek@uj.edu.pl

<sup>1</sup> Astronomical Observatory of Jagiellonian University, Krakow, Poland

## 1. Introduction

Coronal mass ejections (CMEs) play an important role in controlling space weather, which can generate the most intensive geomagnetic disturbances on the Earth (*e.g.*, Gopalswamy *et al.* 2001b, Gopalswamy *et al.* 2002, Gopalswamy 2002; Srivastava and Venkatakrishnan 2002; Kim *et al.* 2005; Moon *et al.* 2005; Manoharan *et al.* 2004; Manoharan 2006; Manoharan 2010; Manoharan and Mujiber Rahman 2011; Shanmugaraju *et al.* 2015). For geomagnetic-storm forecasting it is crucial to predict when a solar disturbance would reach the Earth. This is not an easy task because the rate of expansion of ejections depends on the magnetic force that drives them and the conditions prevailing in the interplanetary medium. In the initial phase, the magnetic force dominates and the ejection is accelerated rapidly. Farther from the Sun, the propelling force weakens and friction begins to dominate. The ejection speed drops gradually approaching the speed of the solar wind. In addition, the ejection velocity can change rapidly as a result of CME–CME interactions. Such collisions mostly occur during a maximum of solar activity.

Initially, models predicting the arrival of interplanetary shocks (IPs) generated by fast CMEs were based on observations of metric Type II radio bursts (Smart and Shea 1985; Smith and Dryer 1990) but these models were inaccurate (Gopalswamy *et al.* 1998; Gopalswamy *et al.* 2001a). Gopalswamy *et al.* (2000a) recognized that the distribution of the speed of interplanetary coronal mass ejections (ICMEs) is much narrower (350–650 km s<sup>-1</sup>) in comparison with the distribution of the speed of CMEs observed near the Sun (150–1050 km s<sup>-1</sup>). This means that CMEs are effectively accelerated as a result of interaction with the solar wind. During expansion, in the interplanetary medium, their speed gradually approaches the speed of the solar wind. Based on these observations, Gopalswamy *et al.* (2000a) introduced an effective acceleration as the difference between the initial [ $u$ ] and final [ $v$ ] speed of an ejection divided by the time [ $t$ ] taken to reach the Earth. They found a definite linear correlation between the effective acceleration [ $a$ ] and initial speed of CMEs:  $a = 1.41 - 0.0035u$  ( $a$  and  $u$  are in units of m s<sup>-2</sup> and km s<sup>-1</sup>, respectively). Gopalswamy *et al.* (2000b) demonstrated that coronagraphic observations are subject to a major projection effect. To estimate this effect, Gopalswamy *et al.* (2001b) used archival data from spacecraft in quadrature (Helios 1 and P78-1). This allowed them to improve the relation between  $a$  and  $u$  ( $a=2.193-0.0054u$ ). This relation was used to predict the arrival time of CMEs at 1 AU. It was demonstrated that the highest accuracy was obtained when the acceleration ceased at a distance of 0.75 AU. Michalek *et al.* (2004) further developed this approach to predicting the 1 AU arrival time of halo CMEs. They proposed to determine the effective acceleration only from two groups of CMEs, the fastest and slowest events. These events are assumed to not have acceleration cessation at any place between the Sun and Earth. To minimize the projection effect they also used an innovative method (Michalek, Gopalswamy, and Yashiro 2003) to obtain the real speed of CMEs. This approach allows one to predict the arrival time of halo CMEs with an average error of 8.7 and 11.2 hours for real and projected initial speeds, respectively.

Another precaution to be taken in determining the TTs of the CMEs concerns the moment when a given event reaches the speed of the solar wind (acceleration cessation). However, estimation of the acceleration cessation distance is not an easy task. Few aerodynamic drag models have been developed to solve this problem (Vršnak *et al.* 2013; Shanmugaraju and Vršnak 2014). These models take into account the difference between speeds of the CMEs and solar wind. Unfortunately, this approach cannot be applied to all CMEs. Using white-light images and interplanetary scintillations, Manoharan (2006) estimated the TTs for 30 CMEs observed from 1998 to 2004. He presented important conclusions showing that the TT can be significantly disturbed by CME–CME interactions and changes in solar-wind properties. Recently Syed Ibrahim, Manoharan, and Shanmugaraju (2017) have studied 51 halo and partial-halo CMEs in the ascending phase of the Solar Cycle 24 and compared the TT relationship with the initial speed of CMEs in the previous solar cycle, Solar Cycle 23 and the current one, Solar Cycle 24. It has been demonstrated that during the present cycle the CMEs have not been significantly affected by the drag force caused by the interplanetary medium.

In our current work, we continue this work using a new approach to a more accurately estimate the TT of the CME. For this purpose, we use images from SOHO *Large Angle and Spectrometric Coronagraphs* (LASCO) and STEREO *Sun Earth Connection Coronal and Heliospheric Investigation* (SECCHI) coronagraphs and employed a new technique to determine the speed of ejections. After the prolonged minimum of Solar Cycle 23, the ascending phase of Solar Cycle 24 was observed starting from 2009 with an increase in the number of CMEs. At the same time, the STEREO spacecraft achieved 90 degrees separation relative to the Earth, a condition known as quadrature. This location of the spacecrafts allows us to give better definition of the parameters of CMEs, especially of those that are directed towards the Earth (halo CMEs). Additionally, in our studies we introduce a new method for determining the speed of ejections that allows us to estimate the instantaneous speed of CMEs.

This article is organized as follows. The data and method used for the study are described in Section 2. In Section 3, we present results of our study. Finally, the conclusions and discussions are presented in Section 4.

## 2. Data and Method

The main aim of the study is to evaluate the TTs of CMEs to the Earth. For this purpose, observations from the two separate spacecrafts, SOHO/LASCO and STEREO/SECCHI, and a new technique to determine the initial speeds of CMEs were employed. Since 1995, CMEs have been routinely recorded by the sensitive LASCO (Brueckner *et al.* 1995) onboard the SOHO mission. The SOHO/LASCO instruments had already recorded about 30,000 CMEs by December 2016. The basic attributes of CMEs, determined manually from running-difference images, among others, are stored in the SOHO/LASCO catalog ([cdaw.gsfc.nasa.gov/CME\\_list](http://cdaw.gsfc.nasa.gov/CME_list), Yashiro *et al.* 2004, Gopalswamy *et al.* 2009). The initial velocity of CMEs obtained by fitting a straight line to the height–time measurements has been

the basic parameter used in prediction of the TT. This catalog has been widely used for different scientific studies. Unfortunately, coronagraphic observations of CMEs are subject to projection effects. This makes it practically impossible to determine the true properties of CMEs and therefore makes it more difficult to forecast their geoeffectiveness. This effect mostly affects geoeffective events that originate from the disk center.

Since the launch of STEREO (Kaiser *et al.* 2008) in 2006 we have a unique opportunity to observe the solar corona from two additional directions. In this study we use these observations to determine velocities of CMEs from additional points of view, since we are concentrating on the events originating in the ascending phase of the Solar Cycle 24. During this period, the STEREO spacecraft were approximately in a quadrature configuration with respect to the Earth. Using quadrature observations with the two STEREO spacecrafts, we can estimate the plane-of-sky speeds which is close to the true radial speed of events ejected from the disk center. This was demonstrated by Bronarska and Michalek (2018). To obtain the STEREO speeds of CMEs we have performed identical manual measurements as in the case of the LASCO observations (Yashiro *et al.* 2014). The only difference was that for these measurements we used COR2 coronagraphs and the optical telescopes: HI1. To determine the speed of a given CME, we employed only images from the STEREO-A or-B spacecrafts, which showed a better quality of observation. This approach allows us to obtain the most accurate height–time data points. As was demonstrated by Michalek, Gopalswamy, and Yashiro (2017) the maximal errors in estimation of velocity significantly depend on the quality of CMEs recorded by LASCO coronagraphs. They also demonstrated that a number of height–time points measured for a particular event is the dominant factor in determining the accuracy of CME parameters to the greatest extent. This number is directly dependent on the quality of observations, instrument data gaps, and CME speed. We must also mention that in the case of our considerations it is not important which STEREO spacecrafts (A or B) observes a given event because our study is carried out in the period when these twin spacecrafts were in quadrature in relation to the Earth. In addition, these studies are concentrated on halo CMEs that are formed in the central part of the solar disk and are directed towards the Earth. Having the STEREO height–time measurements, we could obtain initial speeds of CMEs from a linear fit recorded by instruments onboard the STEREO spacecrafts. These speeds have been calculated in an identical manner, with the exception of the instruments used, as in the case of those included in the SOHO/LASCO catalog.

It is worth emphasizing here why STEREO and SOHO were used to derive speeds separately. In the current research, we focus on halo CMEs. The STEREO observations in quadrature provide speeds that are very close to spatial (real) velocities, whereas measurements with SOHO provide speeds that are significantly modified by projection effects. We are interested in how these different speeds can be used to determine the TT of a CME to the Earth.

Until now, empirical models predicting the TTs of the CMEs have employed the initial velocities of ejections obtained from a linear fit to all manually measured height–time data points. Therefore, the determined speeds are in some

sense the average velocities of CMEs in the field of view of the respective coronagraphs. It is obvious that the instantaneous velocities of CMEs change with distance from the Sun, since initially their speeds increase when their dynamics are dominated by the Lorentz forces, and they reach their maximum speed when the Lorentz force balances the friction force. From this moment, the CMEs are slowed down until they reach the speed of the solar wind. Therefore, it is evident that the speed determined from the linear fit depends not only on the actual CME speed but also on the number of data points and this significantly depends on the brightness of a given ejection.

In this context, it is worthwhile to estimate the CME speed using a different approach, i.e. to determine the initial speed of CMEs based on their maximal velocities. For this approach, in our current work, we employed a simple technique to determine instantaneous velocities of the CMEs. To obtain these velocities we also used linear fits to height–time points but for now we used limited number of these points. In our study we considered linear fits using three to eight height–time data points only. Shifting successively, in this way we can obtain the instantaneous speed of the CME. Using such a linear fit, for all of the height–time data points measured for a given CME, we obtained instantaneous profiles of velocities in time or in distance from the Sun.

From the velocity profiles thus obtained, we can easily determine the maximal velocity, as well as the time and the distance when this speed has been achieved. We tested this method employing different number of height–time points (from three to eight). The most reasonable results were obtained when we employed five successive height–time points for a linear fit, hence we used this method in our present study. Formally, two neighboring height–time points are enough to calculate the instantaneous speed. Unfortunately manual measurements are subject to unpredictable random errors. These errors result from the subjective nature of manual measurements.

In order to minimize the impact of these errors on the determined instantaneous speed we decided to apply linear fits. This technique allows us to obtain smooth profiles of instantaneous speed. Applying this method we have determined profiles of instantaneous velocities of CMEs in the field of view of LASCO (C2 and C3) and STEREO telescopes. In the case of the STEREO twin spacecraft, we used only observations from the one in which the quality of observation was better. We employed subscript <sub>5</sub> to denote that we have used five successive height–time points for linear fit to obtain the maximal velocity. These profiles of instantaneous velocities can be easily used to determine the maximal/  $V_5$  velocity in SOHO ( $V_{5\text{-SOHO}}$ ) and STEREO ( $V_{5\text{-STEREO}}$ ) telescopes. It should be mentioned that these velocities are the plane-of-sky speeds. However,  $V_{5\text{-STEREO}}$  for halo CMEs is very close to the true radial speed. Having the profiles of instantaneous velocities we estimated the time [ $T_{5\text{-SOHO}}$  and  $T_{5\text{-STEREO}}$ ] and distance [ $D_{5\text{-SOHO}}$  and  $D_{5\text{-STEREO}}$ ] when CMEs reached the maximal speeds [ $V_{5\text{-SOHO}}$ ] and STEREO [ $V_{5\text{-STEREO}}$ ] for the respective coronagraphs.

It is obvious that CMEs, when moving from the Sun to the Earth, are subject to three different phases of propagation. First, close to the Sun, they are subject to rapid initial acceleration [phase 1, S1]. At the end of this phase they reach their maximum speeds [ $V_{5\text{-SOHO}}$ ] or STEREO [ $V_{5\text{-STEREO}}$ ]. Then, when their

dynamics is determined by the drag force (due to interaction with solar wind), they move with a negative acceleration [phase 2, S2]. After reaching the speed of the solar wind, they move at a constant speed ( $V_{\text{CONST}}$ , the average speed of the solar wind) until they reach Earth's orbit [phase 3, S3]. Using our definitions we may write:

$$S1 + S2 + S3 = 1\text{AU} \quad (1)$$

$$S1 = D_{5\text{-SOHO}}/D_{5\text{-STEREO}}, \quad (2)$$

where S1, S2, and S3 are the distances that the CME travels in the next three phases of propagation. In our work, we focus only on the last two phases of propagation. During these phases of propagation a given CME traverses the respective distances: we have

$$S2 = V_{\text{MAX}}T2 - \frac{aT2^2}{2} \quad (3)$$

and

$$S3 = V_{\text{CONST}}T3, \quad (4)$$

where  $V_{\text{MAX}}$  is the maximal velocity of CMEs achieved in the respective telescope [ $V_{5\text{-SOHO}}$ ] or [ $V_{5\text{-STEREO}}$ ], T2 is the travel time during the second phase of propagation,  $a$  is acceleration during the second phase of propagation,  $V_{\text{CONST}}$  is the velocity of propagation during the third phase of propagation and T3 is the travel time during the third phase of propagation. These equations form the basis of our further considerations, especially those relating to the TTs of CMEs from the Sun to the Earth. In this approach the TT of a CME is  $T2 + T3$  and the distance to travel is  $S1 + S2$ . These equations fully describe the kinematics of CMEs in the field of view of LASCO and SECCHI coronagraphs. The only undefined parameter is the acceleration [ $a$ ] of CMEs in the second phase of their propagation. Below, we present various methods for its determination. This allows us to test different models used to determine the TTs of CMEs from the Sun to the Earth.

In the paper we consider different methods to determine velocities of CMEs. These velocities can be correlated with the TTs. Fitting curves to TT-velocity points we built theoretical models that can be used to predict the TT in the future. For individual CMEs, we can determine the error in estimation of TT as the difference between the TT determined on the basis of the model and the actual observations. Having these errors for a given model and entire populations of considered CMEs we can determine the average absolute and maximal errors. This means that the maximal error for a given model is the maximal error from the distribution.

### 3. Results

Our study concentrates on the ascending phase of the Solar Cycle 24. During this period we were able to record, at the same time, CMEs observed by

STEREO-A and -B spacecrafts as they were separated by 90 degrees with respect to Earth. Syed Ibrahim, Manoharan, and Shanmugaraju (2017) compiled a list of halo and partial-halo CMEs during 2009-2013. Among them, they were able to identify the ICME at the Earth's vicinity for 51 events. These events are the basis of our study. Their analysis were limited to the data included in the SOHO/LASCO catalog. Additionally, in our research, for each CME included in their list, we conducted the analysis which was described in the previous section. This means that for each CME we have measured height-time points in the STEREO field of view and the initial ejection velocities of CMEs [ $V_{\text{AVG-STEREO}}$  and  $V_{5\text{-STEREO}}$ ] were determined. A few events were too faint in the STEREO images so we were not able to obtain height-time points for them. Having the profiles of instantaneous velocities, we estimated the time and distance when the CMEs reached their maximal speeds. All of these data are shown in Table 1. The near-Sun observational details in the LASCO field of view are given in columns two – seven. The onset date and time of CME ejection are in columns two and three, respectively. The average velocity from a linear fit to all data points (from the SOHO/LASCO catalog), the maximal velocity from linear fit to five successive height-time points, distance, and the time when a given CME reaches the maximal velocity are displayed in column four – seven, respectively. Next, the TTs of ICMEs and shocks and final velocity of ICME in the vicinity of Earth received by the *in-situ* observations made by *AdvancedCompositionExplorer* (ACE) instruments are given in columns eight – ten, respectively. These data are from Syed Ibrahim, Manoharan, and Shanmugaraju (2017). The details from observations in the STEREO field of view are shown in columns eleven – fourteen. In the respective columns we find the average velocity from a linear fit to all data points, the maximal velocity from linear fit to five successive height-time points, distance, and time when a given CME reaches the maximal velocity. The data shown in the table are the basis for our calculation of the TT of CME from the Sun to the Earth. The results are presented in the following sections. In the table are included all CMEs (51) considered by Syed Ibrahim, Manoharan, and Shanmugaraju (2017) having recognised magnetic cloud structure at the Earth (having determined the TT for an ICME). For 48 and 39 (including interacting events) of them we were able to obtain the maximal velocities ( $V_{5\text{-SOHO/STEREO}}$ ) in the SOHO/LASCO and STEREO field of view, respectively.

### 3.1. Velocities of CMEs

In the previous sections, we presented methods for determining the initial speeds of ejections. In this section we present the relationship between these speeds obtained from SOHO and STEREO images. In Figure 1, the successive panels show the relationships between the average and maximal/ $V_5$  speeds determined in SOHO images, the average and maximal/ $V_5$  speeds determined in the STEREO images, the average speeds determined in SOHO and STEREO images and the maximal/ $V_5$  speeds determined in SOHO and STEREO images. Dashed lines are linear fits to data points. Formulas representing linear fits are placed in the lower-right corners of each panel. It can be seen that the average ejection

Table 1.: Observational parameters of 51 ICMEs in the period 2009-2013

#	Date DD/MM/YYYY	Time [HH:MM]	SOHO CME Observations					In-situ Observations				STEREO Observations				
			$V_{AVG}$ [km s <sup>-1</sup> ]	$V_5$ [km s <sup>-1</sup> ]	$R_{MX}$ [R <sub>⊙</sub> ]	$T_{MX}$ [HH:MM]	$TT_{MX}$ [HH]	$TT_{ICME}$ [HH:MM]	$TT_{SHO}$ [HH:MM]	$V_{FIN}$ [km s <sup>-1</sup> ]	$V_{AVG}$ [km s <sup>-1</sup> ]	$V_5$ [km s <sup>-1</sup> ]	$R_{MX}$ [R <sub>⊙</sub> ]	$T_{MX}$ [HH:MM]	$TT_{MX}$ [HH]	
1	16/12/2009	04:30	276	328	10	10:44	132	138:29	134:17	365	416	511	14	09:09	134	
2	07/02/2010	03:54	421	443	13	08:44	94	99:15	93:02	364	418	680	15	07:12	96	
3	12/02/2010	13:42	509	577	14	15:09	77	78:28	77:04	317	637	789	14	14:57	72	
4	12/02/2010	22:30	1180	1387	11	23:49	68	69:16	68:16	317	572	767	14	01:22	68	
5	08/04/2010	04:54	264	315	09	05:30	88	89:00	79:06	423	534	698	55	06:13	87	
6	23/05/2010	18:06	258	340	14	02:44	113	122:07	104:42	383	419	669	13	22:04	118	
7	24/05/2010	14:06	427	490	17	20:44	95	102:07	84:42	383	636	1056	14	18:07	98	
8	22/06/2010	10:50	167	218	07	17:44	87	94:44	87:45	452	-	-	-	-	-	
9	15/02/2011	02:24	669	837	08	03:42	88	90:15	71:14	538	611	1097	06	02:38	90	
10	01/06/2011	18:36	361	507	08	21:54	75	78:18	74:08	520	425	740	80	03:45	78	
11	02/06/2011	08:12	976	1180	19	11:18	62	65:06	60:32	520	650	1324	15	10:07	63	
12	21/06/2011	03:16	719	835	15	04:01	50	51:15	47:09	591	844	1058	25	06:49	47	
13	02/08/2011	06:36	712	936	10	08:06	67	69:35	63:23	404	808	1159	16	08:42	67	
14	03/08/2011	14:00	610	841	05	14:20	64	64:32	51:41	549	1043	1598	15	15:24	63	
15	06/09/2011	02:24	575	-	-	-	-	93:00	82:00	350	695	1246	15	00:51	71	
16	07/09/2011	23:05	792	916	05	23:21	71	71:41	61:05	319	642	810	04	23:08	71	
17	01/10/2011	09:36	448	620	08	11:06	95	97:02	94:02	558	361	737	15	02:42	79	
18	26/12/2011	11:48	736	899	04	12:08	70	70:26	46:16	461	555	906	14	14:22	68	
19	23/01/2012	04:00	2175	2285	23	05:42	41	43:35	34:57	350	1347	2288	14	04:51	42	
20	19/02/2012	20:57	539	736	05	21:40	73	74:20	53:32	577	-	-	-	-	-	
21	07/03/2012	00:24	2684	2789	09	00:49	52	52:17	34:18	500	974	1743	07	00:53	52	
22	07/03/2012	01:30	1825	1946	10	01:54	51	51:23	33:24	717	1151	1552	07	01:38	51	
23	10/03/2012	18:00	1296	1392	12	19:18	50	51:43	39:21	704	1238	2012	14	18:59	50	
24	26/03/2012	23:12	1390	1565	07	23:31	31	32:12	24:12	424	-	-	-	-	-	
25	28/03/2012	01:36	1033	1326	05	02:25	61	62:22	50:23	395	-	-	-	-	-	
26	18/04/2012	09:24	448	669	15	14:06	124	128:06	113:00	384	-	-	-	-	-	
27	18/04/2012	17:24	581	763	06	18:16	120	120:06	105:00	384	407	1130	08	18:38	119	
28	14/06/2012	14:12	987	1151	18	16:54	53	56:34	43:06	515	738	1296	05	14:23	56	
29	28/06/2012	20:00	1313	1570	07	20:25	44	44:34	25:29	660	-	-	-	-	-	
30	02/07/2012	06:24	988	1186	11	08:06	63	65:20	58:23	503	722	842	25	12:49	59	
31	02/07/2012	08:36	1074	1251	12	09:54	61	63:08	56:35	503	-	-	-	-	-	
32	12/07/2012	16:48	885	-	-	17:12	-	62:00	48:00	600	664	1351	07	17:23	61	
33	21/11/2012	16:00	529	807	06	16:49	67	80:11	65:58	410	598	799	15	19:34	64	
34	23/11/2012	13:48	519	680	08	15:49	68	70:18	62:11	517	554	807	16	18:00	65	
35	23/11/2012	23:24	1186	1450	06	23:45	60	60:32	53:13	517	-	-	-	-	-	
36	31/01/2013	06:36	682	925	23	12:18	75	80:05	73:23	444	750	1211	15	09:39	77	
37	06/02/2013	00:24	1867	1923	18	01:37	55	56:15	52:01	419	1084	1652	17	02:33	54	
38	27/02/2013	04:00	622	928	19	10:06	53	59:13	50:46	532	481	682	12	08:55	54	
39	15/03/2013	07:12	1063	1388	18	09:54	53	55:06	46:40	650	669	1382	14	08:51	54	
40	11/04/2013	07:24	861	1099	05	07:45	81	82:13	63:32	457	677	1153	13	09:26	80	
41	21/04/2013	07:24	919	-	-	-	-	71:00	59:00	332	661	949	15	11:21	67	
42	21/04/2013	16:00	857	1113	10	17:30	61	63:21	50:28	332	635	879	05	16:53	62	
43	14/05/2013	23:12	667	1152	05	23:24	87	87:07	73:19	418	736	1049	14	02:54	84	
44	22/06/2013	18:24	477	710	06	19:37	128	141:18	128:17	413	-	-	-	-	-	
45	28/06/2013	02:00	1037	1289	22	02:25	48	49:04	32:37	473	678	1429	08	02:38	48	
46	24/09/2013	20:36	919	1015	05	00:27	46	66:03	53:28	324	-	-	-	-	-	
47	06/10/2013	14:43	567	705	10	17:56	62	120:03	116:13	346	339	1232	11	17:50	62	
48	16/10/2013	15:48	514	623	05	16:32	119	120:44	116:15	304	-	-	-	-	-	
49	24/10/2013	01:25	399	600	04	01:45	113	133:28	129:23	321	292	448	12	06:32	131	
50	07/11/2013	10:36	1405	1712	08	10:55	41	53:31	33:03	603	-	-	-	-	-	
51	28/12/2013	17:36	1118	1247	13	17:52	55	55:26	54:15	423	778	1293	13	19:26	53	



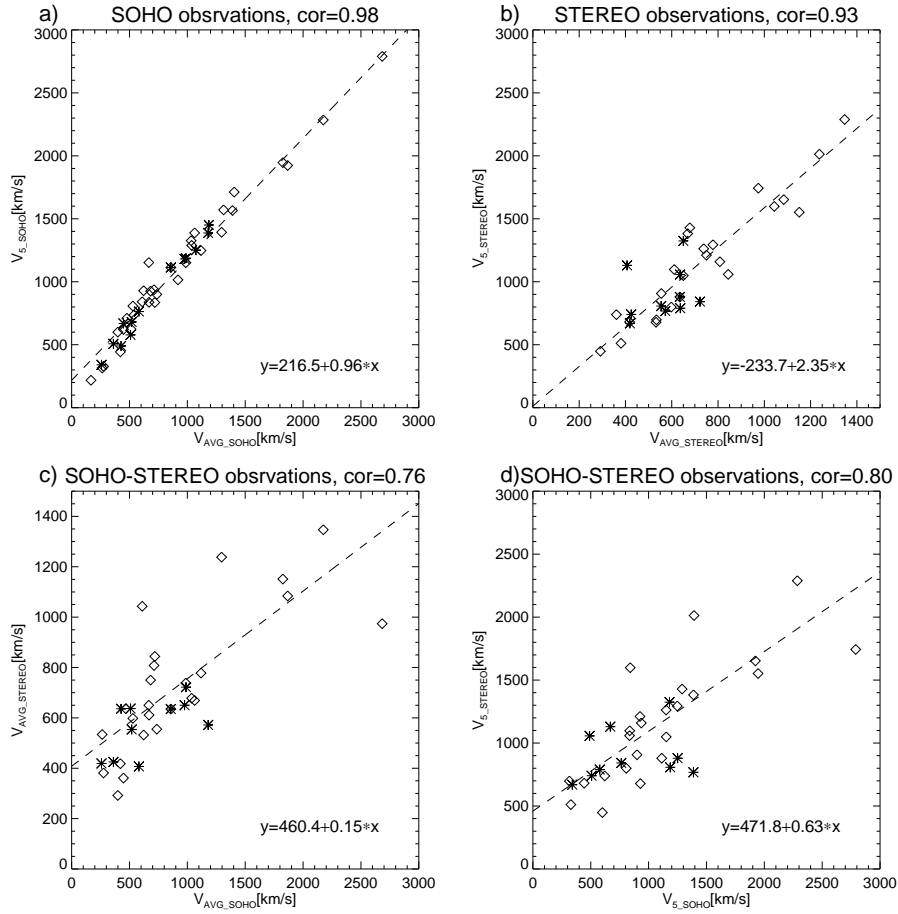


**Figure 1.** Relationship between (a) the average and maximal/ $V_5$  speed determined in SOHO images. (b) the average and maximal/ $V_5$  speed determined in the STEREO images. (c) the average speed determined in SOHO and STEREO images. (d) the maximal/ $V_5$  speed determined in SOHO and STEREO images. *Dashed lines* are linear fits to data points. *Formulas* representing these linear fits are placed in the *lower-right corners* of each panel. *Open diamond symbols* are for non-interacting and *star symbols* are for interacting CME, respectively.

velocities are strongly correlated with their maximal velocities (Panels a and b), regardless of the instrument used for their determination. We can notice that the maximal velocities are much larger (on average 80 %) than the average velocities in the case of observations from the STEREO spacecrafts (Panel b). For SOHO observations the maximal velocities are on average only 25 % larger than the average velocities. This results from the fact that the field of view of STEREO instruments used for determining velocity profiles (COR2 and HI1) is much larger than the field of view of LASCO coronagraphs (C2 + C3). It means that the field of view of the STEREO telescopes covers the area where CMEs undergo significant deceleration due to interaction with the solar wind. For this reason,

the average velocities of the CMEs determined from the STEREO observations are significantly lower than other speeds determined in these studies.

Correlations between the speeds for these two instruments are slightly smaller. The correlation coefficients are 0.75 and 0.80 respectively for the average and maximal speeds. In this case, the larger dispersion of speeds results from the fact that they are determined from the two different instruments (SOHO and STEREO) that observe the Sun at different angles. Depending on the source location on the solar disk and the position of the spacecraft, the determined speeds are subject to different projection effects (Bronarska and Michalek 2018). This effect, among others, is the reason that the determined speeds may be different for each of the telescopes. In our considerations  $V_{5-SOHO}$  are on average smaller (about  $50 \text{ km s}^{-1}$ ) in comparison with  $V_{5-STEREO}$ . This is due to projection effects. Earth-directed CMEs recorded in SOHO/LASCO coronagraphs are subject to more significant projection effects in comparison to observations by the STEREO spacecrafts in a quadrature position.

In Figure 2, relationships between the initial speeds and speeds of interplanetary coronal mass ejections (ICMEs) obtained from *in-situ* measurements are shown. In successive panels we have displayed scatter plots of the average velocities and the maximal/ $V_5$  velocities determined by SOHO and LASCO telescopes *versus* ICME speeds recorded near the Earth.

For the initial speed determined in the SOHO images, the correlation coefficients are less than 0.5. However, in the case of the STEREO spacecraft these correlation coefficients are significantly higher (up to 0.66). It is worth noting that the the most significant correlation is between the final speeds of ICMEs and maximal/ $V_5$  speeds obtained from the STEREO images (Panel d). From the point of view of space weather this is a new and very important result. The speed of an ICME is one of the most important parameters determining the geoeffectiveness of CMEs. These relations for speeds obtained from the STEREO telescopes allow for a more precise estimation of ICME velocities in the vicinity of the Earth and thus the prediction of their impact on the Earth becomes more accurate.

### 3.2. Velocities and Transit Time to the Earth

Depending on the velocity used, in our current research, we define the TT of a CME in two ways. For the average velocities determined in the STEREO or SOHO images, the TT is the time difference between the CME onset time in LASCO-C2 field of view [ $T_{CME}$ ] and the ICME arrival time [ $T_{ICME}$ ] at the Earth's vicinity using *in-situ* observations [ $TT=T_{CME}-T_{ICME}$ ]. In the case of maximal velocities obtained in the STEREO or SOHO images, the TT is the difference between the time when the CME reaches its maximal speed [ $T_{MAX}$ ] and the ICME arrival time [ $T_{ICME}$ ] at the Earth's vicinity using *in-situ* observations [ $TT=T_{MAX}-T_{ICME}$ ]. The TTs for shock generated by ICMEs are obtained in similar ways. The relationships between TTs and CME speeds are shown in the following figures.

As shown in the Figure 3, the TTs for CME with speeds below  $1000 \text{ km s}^{-1}$  are in the range 50-140 hours. The TTs for fast events ( $V>1000 \text{ km s}^{-1}$ ) are

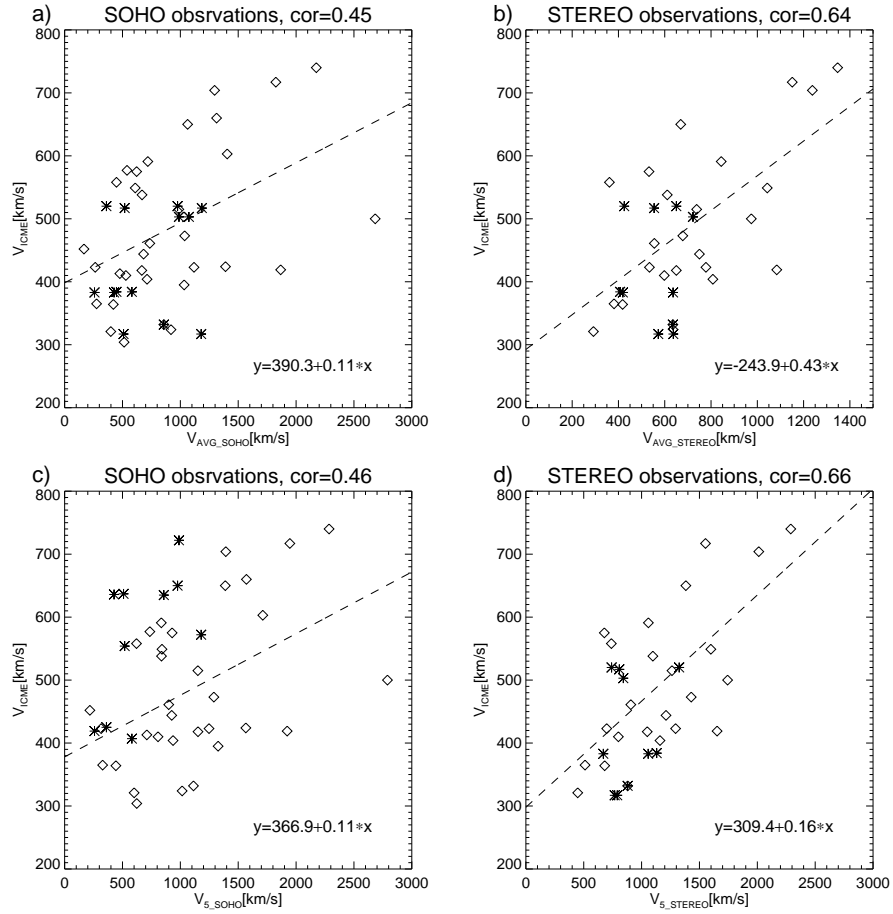


**Figure 2.** The scatter plots of the average and maximal/ $V_5$  speeds determined in SOHO and STEREO images versus ICME speeds determined near the Earth. *Dashed lines* are linear fits to data points. *Formulas* presenting these linear fits are placed in the *lower-left corner of each panel*. *Open diamond symbols* are for non-interacting and *star symbols* are for interacting CMEs, respectively.

in the range 40-60 hours. The third-order polynomial relationship between the observed TT and the speed is indicated by a dashed curve. This fitting can be considered as an empirical model to predict the TT. The difference between the observed and predicted TTs for a given CME speed can be considered as an error by the model. The lower panels show the distribution of errors in determining the TT for this empirical model. The average errors are about  $\approx 11$ -12 hours and the maximum errors are very significant and reach values  $\approx 50$  hours. These errors are the maximum of the distribution of errors. Maximum errors were determined as the maximum difference in time between the theoretical model and the observational data. These errors determined only for non-interacting CMEs.

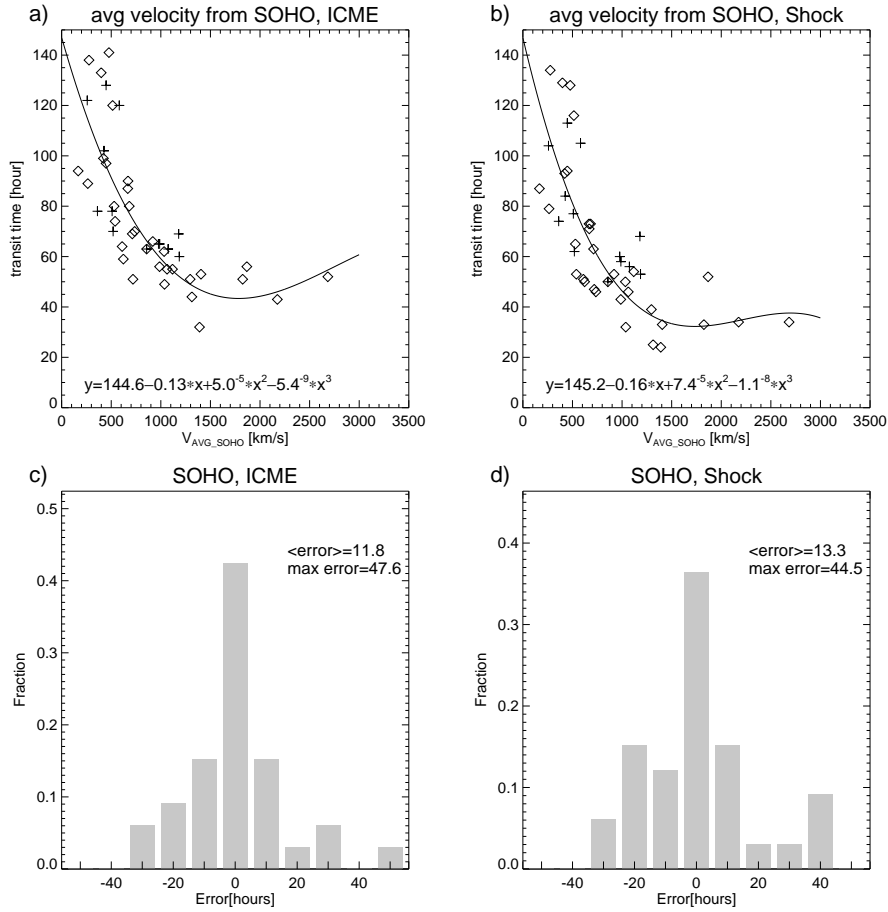


**Figure 3.** Relationship between the average CME speed obtained in the SOHO images and the observed TT for ICME (Panel a) and IP shock (Panel b). *Open diamond symbols* are for non-interacting and *star symbols* are for interacting CMEs, respectively. The third-order polynomial relationship between the observed TT and the speed is indicated by a *dashed curve*. The distributions of errors between predicted and observed TTs are presented in bottom panels (Panel c for ICME and Panel d for IP shock). The values of average and maximal errors are presented in the panels.

In Figure 4 we display the same data but for the maximal velocity/ $V_5$  obtained from the SOHO images. As shown in the figure, results are similar but the average errors are slightly higher,  $\approx 13$  hours. This means that the introduction of the maximal velocity of CME has no effect on a more accurate TT prediction. Figures 3 and 4 and the above discussion refer to SOHO observations.

In Figure 5, results for the average speeds determined in the STEREO images are presented. As shown in the figure, the TT is significantly related to the average speed. The data points are not scattered around the empirical model represented by a third-order polynomial fit. This fit is represented by a dashed curve. This empirical model can be used, with great accuracy, to predict TTs of

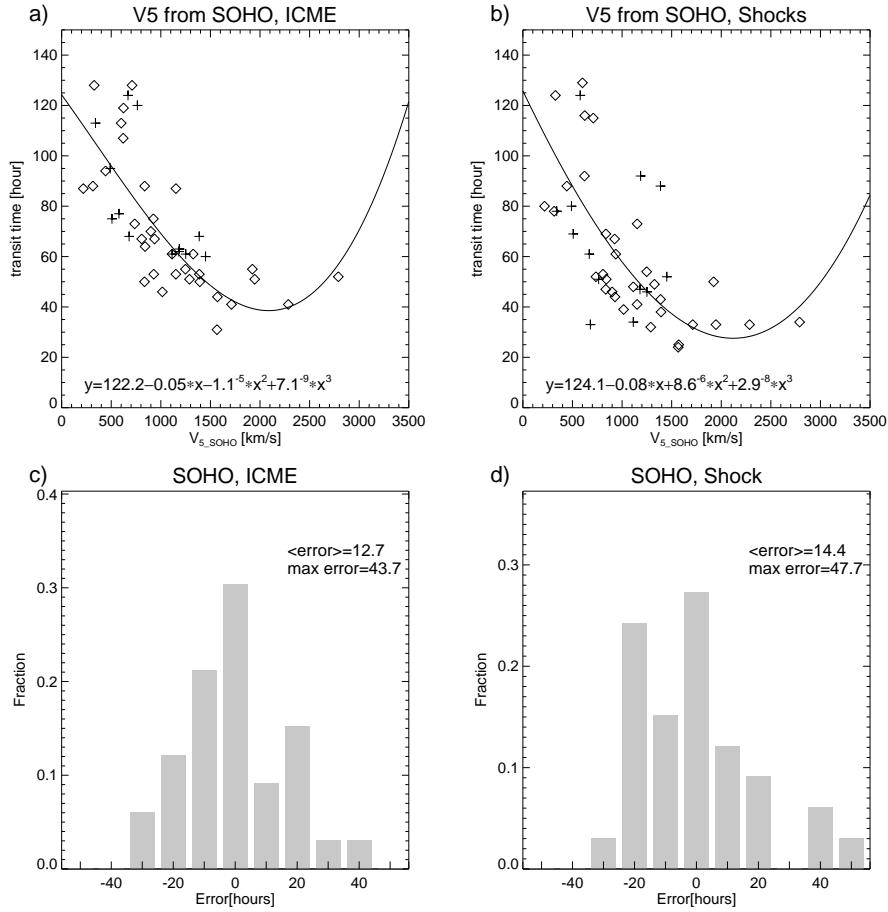


**Figure 4.** Relationship between the maximal/ $V_5$  CME speed and the observed TT for ICME (Panel a) and IP shock (Panel b). *Open diamond* symbols are for non-interacting and *star symbols* are for interacting CMEs, respectively. The third-order polynomial relationship between the observed TT and the speed is indicated by a *dashed curve*. The distributions of errors between predicted and observed TTs are presented in bottom panels (Panel c for ICME and Panel d for IP shock). The values of average and maximal errors are presented in the panels.

CMEs. In this case the average errors in the prediction of the TT are only  $\approx 9$  and 10 hours for ICMEs and IP shock, respectively. However, a more significant fact is that in this case the maximal errors are much lower than in the previously presented models (Gopalswamy *et al.* 2001b, Michałek *et al.* 2004; Manoharan 2006), i.e. 29 and 38 hours for ICME and IP shock, respectively. Similar results were obtained for the maximal/ $V_5$  speed in the STEREO images. Results for these considerations are shown in Figure 6.

It is also worth mentioning that in the case of fast CMEs ( $V > 1200 \text{ km s}^{-2}$ ), the empirical model is a better approach in predicting TTs. For these events, average errors are below five hours and the maximal error does not exceed ten

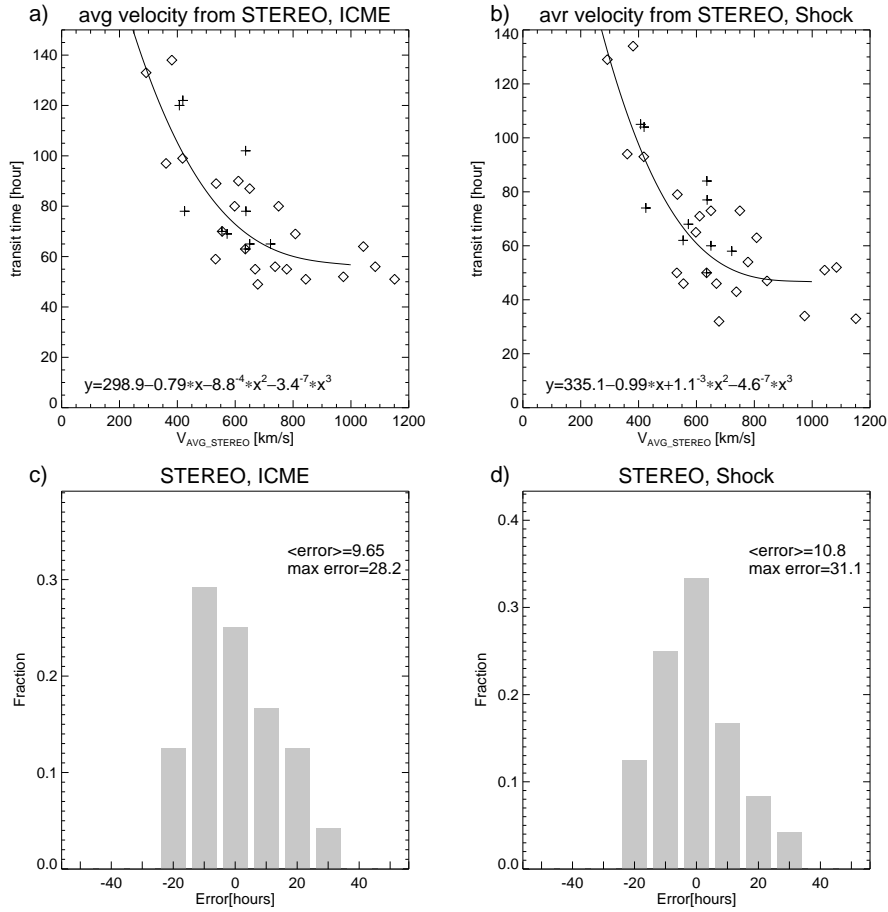


**Figure 5.** Relationship between the average CME speed obtained from the STEREO images and the observed TT for ICME (Panel a) and IP shock (Panel b). *Open diamond symbols* are for non-interacting and *star symbols* for interacting CMEs, respectively. The third-order polynomial relationship between the observed TT and the speed is indicated by a *dashed curve*. The distributions of errors between predicted and observed TT are presented in bottom panels (Panel c for ICME and Panel d for IP shock). The values of average and maximal errors are presented in the panels.

hours. This is illustrated in the figure by two additional dashed curves showing a deviation from the model of  $\pm$ ten hours.

### 3.3. CME Transit Time Estimation

Having determined the different initial velocities (maximal or average), we are able to calculate TTs directly using kinematic equations of motion. For this purpose, we assume that once the CME reaches the initial velocity it moves with an uniform negative acceleration. This movement is controlled by drag force due to interaction with the solar wind. Deceleration stops when the CME speed reaches that of the solar wind (i.e. 300-400 km s<sup>-1</sup>). From this moment

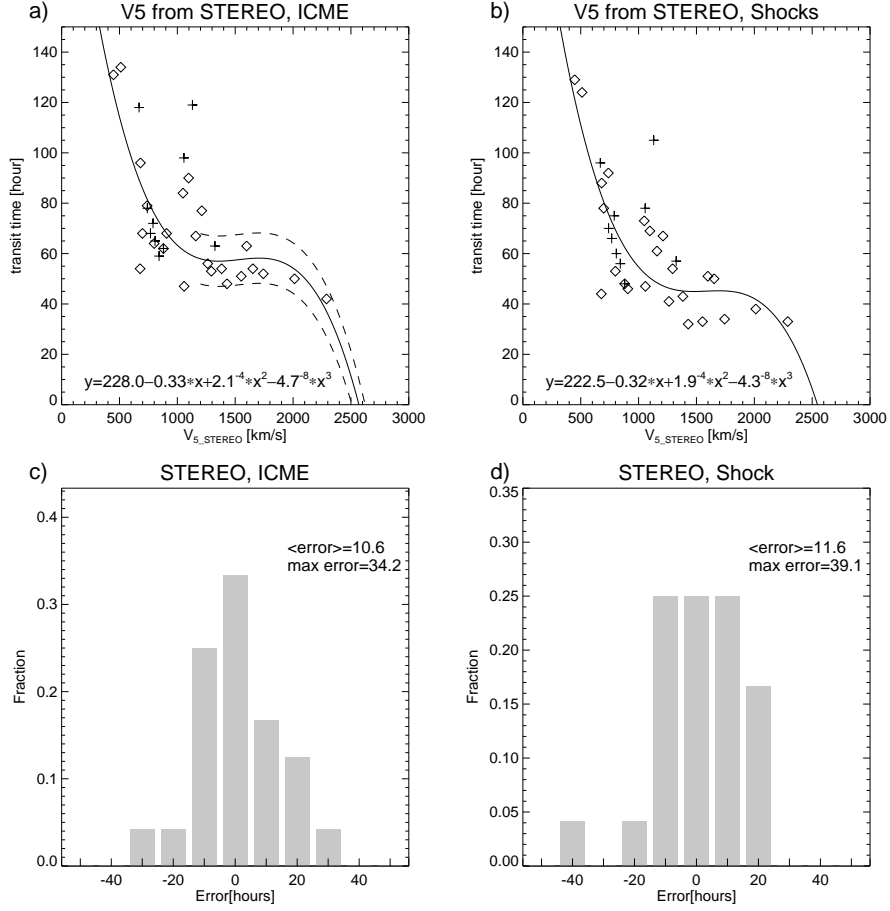


**Figure 6.** Relationship between the maximal/ $V_5$  CME speed obtained from the STEREO images and the observed TT for ICME (Panel a) and IP shock (Panel b). *Open diamond* symbols are for non-interacting and *star symbols* are for interacting CMEs, respectively. The third-order polynomial relationship between the observed TT and the speed is indicated by a *dashed curve*. The distributions of errors between predicted and observed TTs are presented in bottom panels (Panel c for ICME and Panel d for IP shock). The values of average and maximal errors are presented in the panels. Two additional *dashed lines* illustrate deviation from the model of  $\pm 10$  hours.

onwards the CME moves with constant velocity, which is recorded at the Earth [ $V_{\text{FINAL}}$ ]. Knowing the acceleration and using the above assumptions, we can easily calculate TT. The data we have allows us to determine the effective acceleration of CMEs (Gopalswamy *et al.* 2001b). They are designated as the quotient of the speed difference determined in the vicinity of the Sun and that determined at the Earth's vicinity over the TTs of CMEs. It can be expressed by the equation

$$ACC_{\text{EFFECTIVE}} = (V_{\text{INITIAL}} - V_{\text{FINAL}})/TT, \quad (5)$$

where  $V_{\text{INITIAL}}$  is velocity of CME determined near the Sun (average or maximal/ $V_5$ ) and  $V_{\text{FINAL}}$  is velocity of ICME measured at the Earth's vicinity and TT, is the transit time of a given CME that is defined in the previous sections.

The relationship between initial velocities ( $V_{\text{AVG-SOHO}}$ ,  $V_{5\text{-SOHO}}$ ,  $V_{\text{AVG-STEREO}}$ ,  $V_{5\text{-STEREO}}$ ) of CMEs and their effective accelerations are shown in Figure 7. The quadratic relationship between the effective accelerations and the respective speeds are indicated by a solid line. These curves represent empirical models of effective acceleration of CMEs depending on their initial speeds. Michalek *et al.* (2004) demonstrated that the average acceleration models cannot give accurate prediction of TTs. They proposed to introduce the effective acceleration of a CME which is computed using a linear fit to two extreme samples of CMEs. The slowest events which have no acceleration and the fastest events are accelerated up to 1 AU. These events are expected to have no acceleration cessation during their travel to the Earth (Michalek *et al.* 2004). The dashed lines, in Figure 7 are linear fits to the these groups of CMEs only.

With the help of different CME acceleration empirical models, we are able to determine the TT using general equations of motion. The results are displayed in Figures 8 and 9. The scatter plots below display the observed *versus* predicted TT for the respective acceleration models displayed in Figure 7, which also shows a comparison of TTs for SOHO observations. Unfortunately, the results are not very accurate. Average errors for models obtained from the average and maximal speeds are above 13 and 15 hours, respectively.

As seen from the figure, the results seem to be better for effective accelerations determined from linear fits (Panels b and d) in comparison to those received from quadratic fits (Panels a and c). For the effective acceleration models obtained from the average velocities, data points are symmetrically scattered around the solid line, that shows the ideal situation when both times are equal. In the case of the maximal velocities the data points are mostly placed below this line. This means that on average the predicted TT are lower than observed TT.

In Figure, we have similar comparisons but for STEREO observations. In this case the results are more promising. For all of the models considered, the average errors are  $\approx 9\text{--}12$  hours. However, the best results are for the effective acceleration obtained from the average velocities (Panels a and b). As seen from the figures, the average and maximal errors are smallest and the symmetric scatter of data points around the solid line represents the ideal situation when observed and predicted TT are equal.

### 3.4. Errors *Versus* the Range of CME Observation from the Sun

The results obtained show that the best accuracy in predicting TT are provided by models based on the average speed determined from the STEREO observations (Figure 5a and Figure 9b). Using these two models the predicted TT are subject to minimal (9.27 hours, 10.2 hours) and maximal (28.3 hours, 26.6 hours) errors, respectively.

It is important to consider why these observations provide the best results. Certainly, the direction of observation has some influence. It seems that observations from the STEREO spacecraft, in the case of a CME directed toward



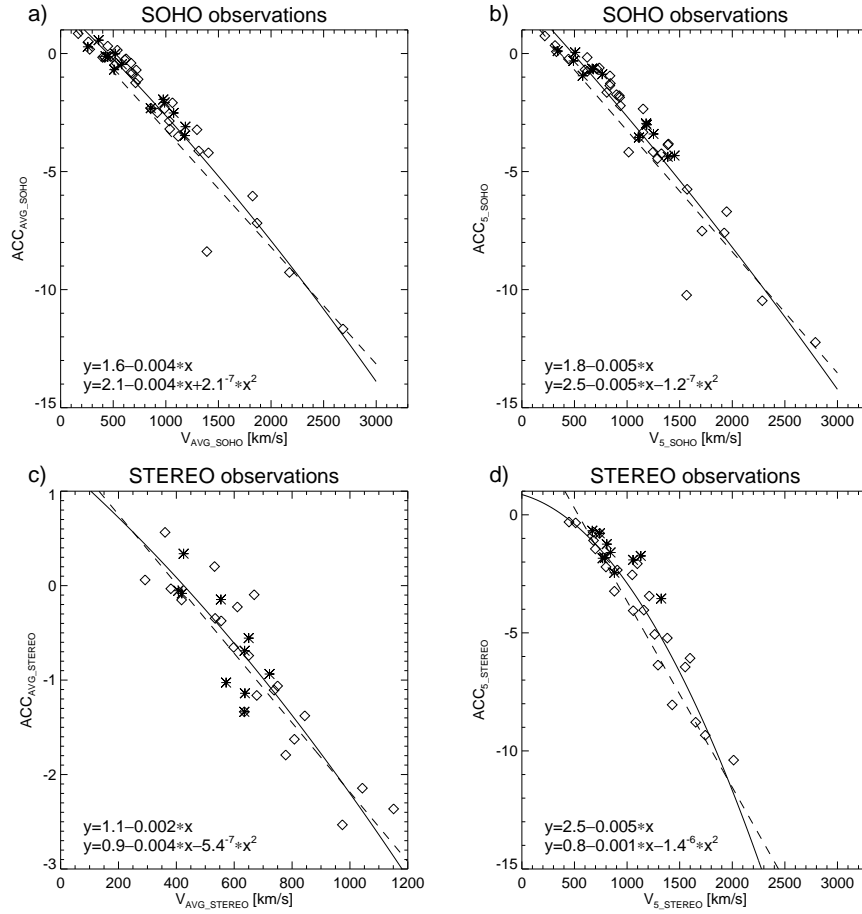


**Figure 7.** Scatter plots of effective acceleration versus respective initial speed of CMEs [ $V_{AVG-SOHO}$ ,  $V_{5-SOHO}$ ,  $V_{AVG-STEREO}$ ,  $V_{5-STEREO}$ ]. The *open diamond symbols* are for non-interacting and *star symbols* for interacting CMEs. The *solid curves* are quadratic fits to the data points. The *dashed lines* are linear fits for the three slowest and the three fastest events from the entire sample of CMEs.

the Earth, are subject to smaller projection effects than those conducted with the SOHO spacecraft. However, another important factor to be considered is the field of view of the STEREO telescopes, which is much larger than the field of view of the SOHO coronagraphs. This effect is illustrated in Figure 10. This figure shows scattered plots of the difference between predicted (errors of predictions) and observed TT *versus* range of observations of CME [ $D_{MAX}$ ]. The parameter [ $D_{MAX}$ ] is the maximal distance where a given CME was recorded by the STEREO telescopes. The left panel presents the results for the empirical model shown in Figure 5a and the right panel presents the results for calculation displayed in Figure 9a. As shown here, the errors in prediction depends on the range of observations. The correlation coefficients are  $\approx 0.5$ . This result is consistent with considerations presented by Bronarska and Michalek (2018).

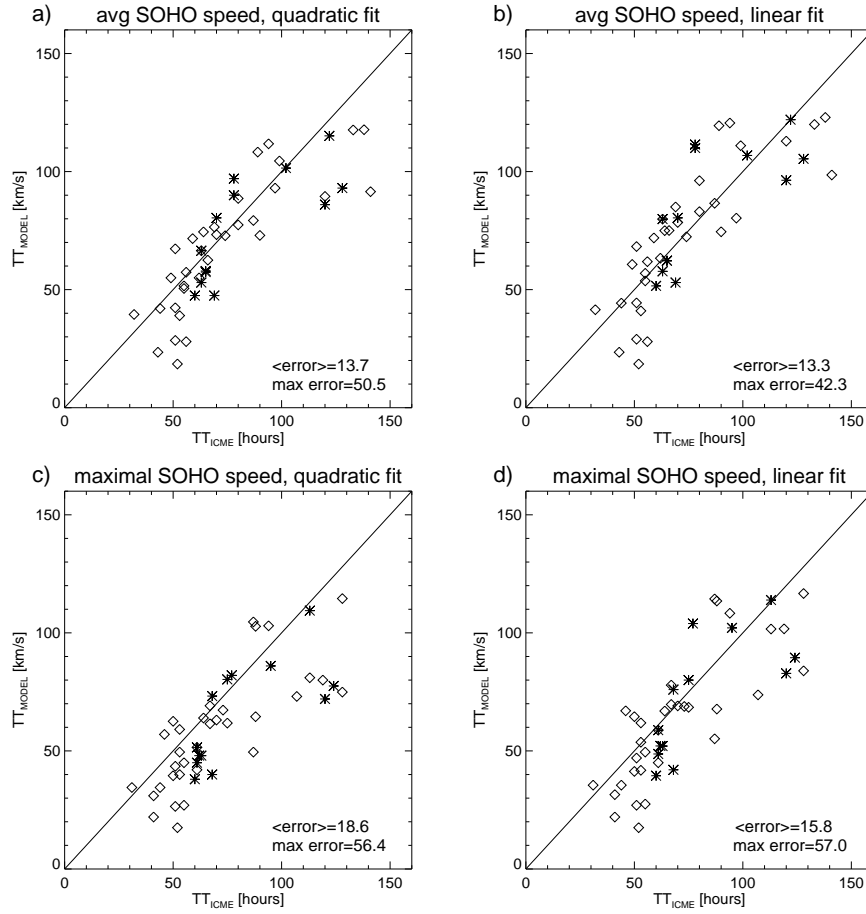


**Figure 8.** Scatter plots presenting comparison between observed and predicted TT based on acceleration profiles obtained from SOHO observations. In the respective panels we have results for effective acceleration obtained from a quadratic fit (Panels **a** and **b**) and from a linear fit (Panels **c** and **d**). The *upper panels* are for effective acceleration obtained from the average velocities and the bottom from the maximal/ $V_5$  velocities, respectively. The *open diamond symbols* are for non-interacting and *star symbols* for interacting CMEs. *Solid lines* show the theoretical situation when observed and predicted times are identical.

They showed that the errors in determining the speed depend, to the highest degree, on the number of height–time points. The average speeds determined from the STEREO observation have the highest number of height–time points and are therefore determined with the best accuracy.

#### 4. Summary and Discussion

In this study we evaluate the TT of CMEs during the ascending phase of Solar Cycle 24. For this purpose we employed, different from the previous studies, two additional STEREO coronagraphs observing the Sun in quadrature and provided

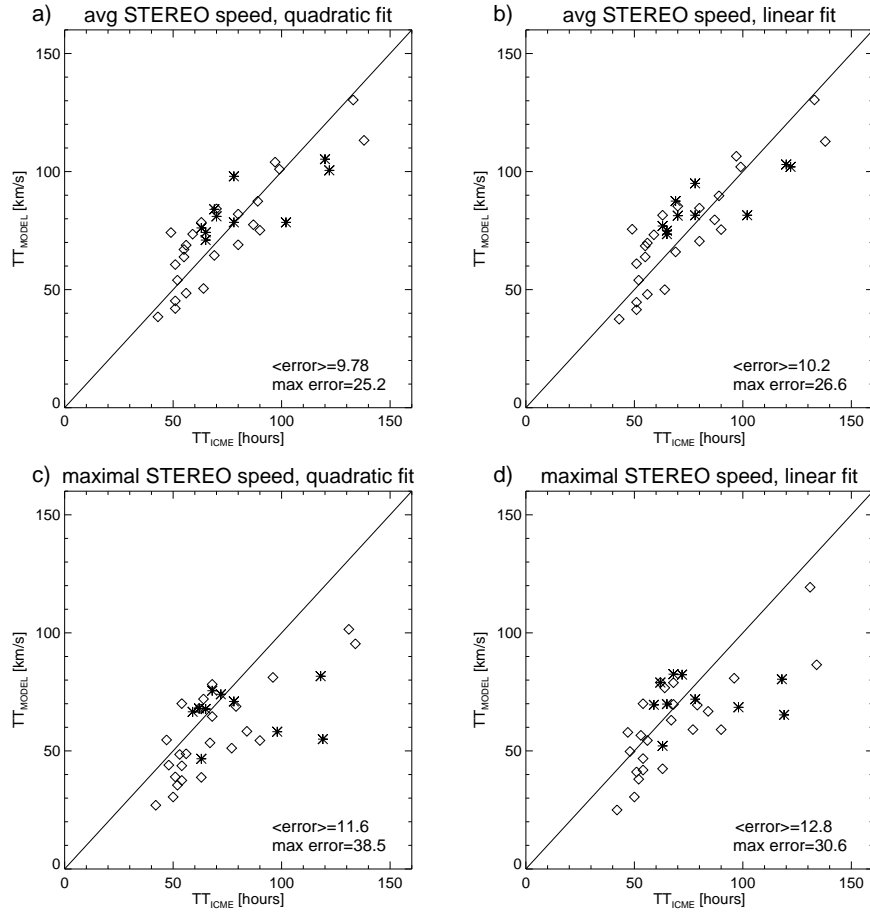


**Figure 9.** Scatter plots showing comparison between observed and predicted TT based on acceleration profiles obtained from the STEREO observations. In the respective panels we have results for effective acceleration obtained from a quadratic fit (Panels **a** and **b**) and from a linear fit (Panels **c** and **d**). The *upper panels* are for effective acceleration obtained from the average velocities and the bottom from the maximal/ $V_5$  velocities, respectively. The *open diamond symbols* are for non-interacting and *star symbols* for interacting CMEs. *Solid lines* show the theoretical model when observed and predicted TT are identical.

a new definition of initial speed of CMEs. It was demonstrated that all the considered initial speeds [ $V_{AVG-SOHO}$ ,  $V_{5-SOHO}$ ,  $V_{AVG-STEREO}$ ,  $V_{5-STEREO}$ ] are significantly correlated, however, the most significant correlation appears to be between the velocities determined using the same spacecrafts. The maximal velocities are larger by about 80% and 25% than the average velocities for the STEREO and SOHO telescopes, respectively. The initial velocities determined in the STEREO images [ $V_{AVG-STEREO}$ ,  $V_{5-STEREO}$ ] are also significantly related to the final velocities of an ICME. This is a very important result from the point of view of space weather. This allows us to accurately predict one of the most important parameter determining geoeffectiveness of CMEs.

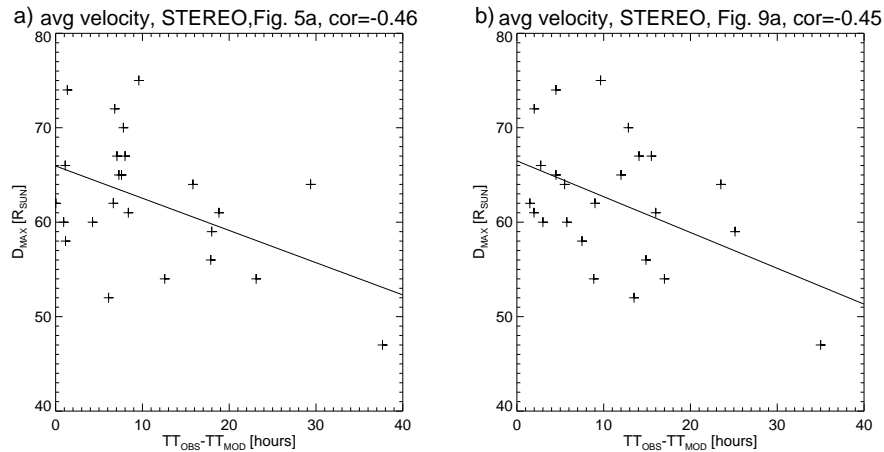


**Figure 10.** Scatter plots of difference between predicted (errors of predictions) and observed TT versus range of observations of CME [ $D_{MAX}$ ]. The *left panel* presents the results for the empirical model shown in Figure 5a and the *right panel* presents the results for calculations displayed in Figure 9a.

The TT of CMEs to the Earth is the next important parameter for space weather. We presented two methods, using the initial velocities of CMEs estimated near the Sun, to predict the TT. First, we used the correlation between the initial velocities and the TT to generate empirical models predicting the TT. The best empirical models are for the average speeds estimated in the STEREO images (Figure 4a). Second, we calculated the TT using kinematic equations of motions and different models of effective acceleration. Again the best results were obtained for average velocities determined in the STEREO field of view (Figure 9a).

Using observations from the STEREO we were able to reduce the average absolute errors of TT prediction by only about an hour. However, what is more important is the fact that the new approach have radically reduced the maximum TT estimation errors equal to 29 hours. Previous studies determined the TT with the maximum error equal 50 hours. We also tried to find out why the STEREO observations are more useful in determining the TT. As the STEREO field of view is much larger than SOHO field of view, it allows us to follow the CME up to one third of the way to the Earth and thus more accurately determine their speed. It is shown that errors in predicting TT significantly depend on the distance range of the CME observation, i.e. the larger the observation range, the smaller the error.

In our research we defined a new initial velocity of a CME, the maximum velocity determined from the velocity profiles obtained from a moving linear fit to five consecutive height–time points. This new approach have radically reduced the maximum TT errors equal to 29 hours. Previous studies determined the TT with the maximum error equal 50 hours. Additionally, the maximal velocities of CMEs are better correlated with the final ICME speeds in comparison with previous models. It is also worth noting that in the case of maximum speeds,

the empirical model obtained from the correlation between these speeds and TT are in good agreement. Results for these considerations are shown in Figure 6. For the fast CMEs ( $V > 1200 \text{ km s}^{-1}$ ), the empirical model works very well, as the average errors are below five hours and the maximal error does not exceed ten hours.

The model presented can be used universally. As input to this model, we can use speeds or accelerations obtained in different ways. In particular, we can use the real three dimensional speeds estimated using stereoscopic observation from all of the coronagraphs. It seems, however, that the results obtained in this way will not be significantly different from those obtained from the STEREO observations. As we mentioned earlier, STEREO observations in quadrature, in the case of halo CMEs, provide velocities very close to the real ones.

### Acknowledgements

Anitha Ravishankar and Grzegorz Michalek were supported by NCN through the grant UMO-2017/25/B/ST9/00536.

## 5. Disclosure of Potential Conflicts of Interest

The authors declare that they have no conflicts of interest.

## References

- Bronarska, K., Michalek, G.: 2018, Determination of projection effects of CMEs using quadrature observations with the two STEREO spacecraft. *Adv. Space Res.* **62**, 408. DOI. ADS.
- Brueckner, G.E., Howard, R.A., Koomen, M.J., Korendyke, C.M., Michels, D.J., Moses, J.D., Socker, D.G., Dere, K.P., Lamy, P.L., Llebaria, A., Bout, M.V., Schwenn, R., Simnett, G.M., Bedford, D.K., Eyles, C.J.: 1995, The Large Angle Spectroscopic Coronagraph (LASCO). *Solar Phys.* **162**, 357. DOI. ADS.
- Gopalswamy, N.: 2002, Relation Between Coronal Mass Ejections and their Interplanetary Counterparts. In: Wang, H., Xu, R. (eds.) *Solar-Terrestrial Magnetic Activity and Space Environment* **14**, 157. ADS.
- Gopalswamy, N., Kaiser, M.L., Lepping, R.P., Kahler, S.W., Ogilvie, K., Berdichevsky, D., Kondo, T., Isobe, T., Akioka, M.: 1998, Origin of coronal and interplanetary shocks: A new look with WIND spacecraft data. *J. Geophys. Res.* **103**, 307. DOI. ADS.
- Gopalswamy, N., Lara, A., Lepping, R.P., Kaiser, M.L., Berdichevsky, D., St. Cyr, O.C.: 2000a, Interplanetary acceleration of coronal mass ejections. *Geophys. Res. Lett.* **27**, 145. DOI. ADS.
- Gopalswamy, N., Kaiser, M.L., Thompson, B.J., Burlaga, L.F., Szabo, A., Lara, A., Vourlidas, A., Yashiro, S., Bougeret, J.-L.: 2000b, Radio-rich solar eruptive events. *Geophys. Res. Lett.* **27**, 1427. DOI. ADS.
- Gopalswamy, N., Yashiro, S., Kaiser, M.L., Howard, R.A., Bougeret, J.-L.: 2001a, Characteristics of coronal mass ejections associated with long-wavelength type II radio bursts. *J. Geophys. Res.* **106**, 29219. DOI. ADS.
- Gopalswamy, N., Lara, A., Yashiro, S., Kaiser, M.L., Howard, R.A.: 2001b, Predicting the 1-AU arrival times of coronal mass ejections. *J. Geophys. Res.* **106**, 29207. DOI. ADS.

- Gopalswamy, N., Yashiro, S., Michalek, G., Kaiser, M.L., Howard, R.A., Reames, D.V., Leske, R., von Roseninge, T.: 2002, Interacting Coronal Mass Ejections and Solar Energetic Particles. *Astrophys. J.* **572**, L103. DOI. ADS.
- Gopalswamy, N., Yashiro, S., Michalek, G., Stenborg, G., Vourlidas, A., Freeland, S., Howard, R.: 2009, The SOHO/LASCO CME Catalog. *Earth Moon and Planets* **104**, 295. DOI. ADS.
- Kaiser, M.L., Kucera, T.A., Davila, J.M., St. Cyr, O.C., Guhathakurta, M., Christian, E.: 2008, The STEREO Mission: An Introduction. *Space Sci. Rev* **136**, 5. DOI. ADS.
- Kim, R.-S., Cho, K.-S., Moon, Y.-J., Kim, Y.-H., Yi, Y., Dryer, M., Bong, S.-C., Park, Y.-D.: 2005, Forecast evaluation of the coronal mass ejection (CME) geoeffectiveness using halo CMEs from 1997 to 2003. *J. Geophys. Res* **110**, A11104. DOI. ADS.
- Manoharan, P.K.: 2006, Evolution of Coronal Mass Ejections in the Inner Heliosphere: A Study Using White-Light and Scintillation Images. *Solar Phys.* **235**, 345. DOI. ADS.
- Manoharan, P.K.: 2010, Solar cycle changes of large-scale solar wind structure. In: Kosovichev, A.G., Andrei, A.H., Rozelot, J.-P. (eds.) *Solar and Stellar Variability: Impact on Earth and Planets, IAU Symposium* **264**, 356. DOI. ADS.
- Manoharan, P.K., Mujiber Rahman, A.: 2011, Coronal mass ejections—Propagation time and associated internal energy. *J. Atmos. Solar-Terr. Phys.* **73**, 671. DOI. ADS.
- Manoharan, P.K., Gopalswamy, N., Yashiro, S., Lara, A., Michalek, G., Howard, R.A.: 2004, Influence of coronal mass ejection interaction on propagation of interplanetary shocks. *J. Geophys. Res* **109**, A06109. DOI. ADS.
- Michalek, G., Gopalswamy, N., Yashiro, S.: 2003, A New Method for Estimating Widths, Velocities, and Source Location of Halo Coronal Mass Ejections. *Astrophys. J.* **584**, 472. DOI. ADS.
- Michalek, G., Gopalswamy, N., Yashiro, S.: 2017, CME Velocity and Acceleration Error Estimates Using the Bootstrap Method. *Solar Phys.* **292**, 114. DOI. ADS.
- Michalek, G., Gopalswamy, N., Lara, A., Manoharan, P.K.: 2004, Arrival time of halo coronal mass ejections in the vicinity of the Earth. *Astron. Astrophys.* **423**, 729. DOI. ADS.
- Moon, Y., Cho, K., Dryer, M., Kim, Y., Bong, S., Chae, J., Park, Y.: 2005, New Geoeffective Parameters of Very Fast Halo Coronal Mass. *AGU Spring Meeting Abstracts*, SH23A. ADS.
- Shanmugaraju, A., Vršnak, B.: 2014, Transit Time of Coronal Mass Ejections under Different Ambient Solar Wind Conditions. *Solar Phys.* **289**, 339. DOI. ADS.
- Shanmugaraju, A., Syed Ibrahim, M., Moon, Y.-J., Mujiber Rahman, A., Umapathy, S.: 2015, Empirical Relationship Between CME Parameters and Geo-effectiveness of Halo CMEs in the Rising Phase of Solar Cycle 24 (2011 - 2013). *Solar Phys.* **290**, 1417. DOI. ADS.
- Smart, D.F., Shea, M.A.: 1985, A simplified model for timing the arrival of solar flare-initiated shocks. *J. Geophys. Res* **90**, 183. DOI. ADS.
- Smith, Z., Dryer, M.: 1990, Magnetohydrodynamic Study of Temporal and Spatial Evolution of Simulated Interplanetary Shocks in the Ecliptic Plane Within 1-A.U. *Solar Phys.* **129**, 387. DOI. ADS.
- Srivastava, N., Venkatakrisnan, P.: 2002, Relationship between CME Speed and Geomagnetic Storm Intensity. *Geophys. Res. Lett.* **29**, 1287. DOI. ADS.
- Syed Ibrahim, M., Manoharan, P.K., Shanmugaraju, A.: 2017, Propagation of Coronal Mass Ejections Observed During the Rising Phase of Solar Cycle 24. *Solar Phys.* **292**, 133. DOI. ADS.
- Vršnak, B., Žic, T., Vrbanec, D., Temmer, M., Rollett, T., Möstl, C., Veronig, A., Čalogović, J., Dumbović, M., Lulić, S., Moon, Y.-J., Shanmugaraju, A.: 2013, Propagation of Interplanetary Coronal Mass Ejections: The Drag-Based Model. *Solar Phys.* **285**, 295. DOI. ADS.
- Yashiro, S., Gopalswamy, N., Michalek, G., St. Cyr, O.C., Plunkett, S.P., Rich, N.B., Howard, R.A.: 2004, A catalog of white light coronal mass ejections observed by the SOHO spacecraft. *J. Geophys. Res* **109**, A07105. DOI. ADS.
- Yashiro, S., Gopalswamy, N., Akiyama, S., Makela, P.A., Xie, H.: 2014, Association Rate of Major Sep Events As a Function of CME Speed and Source Longitude. In: *AGU Fall Meeting Abstracts* **2014**, SH43A. ADS.